

Model agnostic local variable importance for locally dependent relationships

Kelvyn K. Bladen* Adele Cutler* D. Richard Cutler* Kevin R. Moon*

Abstract

Global variable importance measures are commonly used to interpret the results of machine learning models. Local variable importance techniques assess how variables contribute to individual observations. Current methods typically fail to accurately reflect locally dependent relationships between variables and instead focus on marginal importance values. Additionally, they are not natively adapted for multi-class classification problems. We propose a new model-agnostic method for calculating local variable importance, CLIQUE, that captures locally dependent relationships, improves over permutation-based methods, and can be directly applied to multi-category classification problems. Simulated and real-world examples show that CLIQUE emphasizes locally dependent information and properly reduces bias in regions where variables do not affect the response.

1 Introduction

Variable importance measures are essential for interpreting machine learning models, as they evaluate the relative importance of each feature in the trained model. In particular, global variable importance methods quantify this importance for an entire dataset and have been researched extensively. Breiman [4] introduced a global permutation technique for an internal validation set within Random Forests. This concept was later generalized to model-agnostic approaches [8]. Other global variable importance methods include leave-one-covariate-out (LOCO) [15, 12, 3], knockoffs [2, 5], and using the spread of predictions in partial dependence plots (PDPs) [10, 11]

Local variable importance seeks to measure the relative importance of each feature for individual observations. Existing methods include ICE [9], LIME [24], Counterfactual Explanations [27, 7], Anchors [25], Shapley values [26], and SHAP [17]. SHAP and LIME are particularly popular because of their theoretical foundations, applications to a variety of data types, and their intuitive results [19]. SHAP values are calcu-

lated by considering coalitions of feature values. This involves changing the value of a given variable for a given observation, while allowing other variables to change, and observing the impact on prediction. The average change in prediction across all coalitions yields the SHAP value. Because this allows other variables to change, SHAP values can capture effects that are not only marginal, but sometimes even interactive. However, our experiments show that individual SHAP values do not always capture local interactions effectively.

LIME [24] is another local method which uses interpretable models such as linear regression or classification trees to explain individual predictions of black-box models. LIME creates a new dataset of perturbed features (noise added), where the black-box predictions become the response [19]. An interpretable model is built on the new dataset, weighted by proximity to a given observation of interest. The local importances for that observation are then computed from the global variable importances for the interpretable model. The resulting output requires many simple models: one for each observation. The variables in the models have weights and can be used to create a matrix of weights or importances. We show in our experiments that LIME tends to focus almost entirely on marginal variable importances and fails to detect variable interactions.

In the ICE method, developed by Goldstein et al. [9], a model is built to relate a response to features. Variables are sequentially evaluated by systematically replacing each observation value with values from a uniform grid that ranges from the minimum to the maximum value of the variable. Although a uniform grid is typical, CLIQUE employs the more robust quantile grid technique. In ICE, predictions are then generated for each grid value. ICE plots are created by plotting the predictions across the grid values in a line graph, where each line represents an observation from the dataset. Molnar [19] points out that ICE plots are inherently local and are often insightful when dealing with variable interactions. However, ICE plots do not natively produce a single measure of variable importance.

Compared to other local importance techniques, SHAP and LIME stand out because they produce an

*Department of Mathematics and Statistics, Utah State University

importance value for every value in a data set. For this reason, we will focus primarily on comparing our results with those of SHAP and LIME. We demonstrate in our experiments that SHAP and LIME values often yield nonzero importances in regions of the data where a variable should have no impact on the response. This can lead to inaccurate interpretations where locally unimportant variables are falsely characterized as important. Generalizing these methods to multi-category classification tasks is also challenging. This is because they focus on predictions, which requires developing importances for each individual response class.

To address these limitations, we propose a new approach for assessing local variable importance that we call Conditional Local Importance by QUantile Expectations (CLIQUE). CLIQUE converts global permutation techniques to a local method by addressing individual cross-validation errors rather than the average error. It also uses quantile replacements rather than random permutations, which require far more repetitions to converge. Since CLIQUE computes importances based on the errors instead of the predictions, it can be easily applied to multi-class problems. In contrast to SHAP and LIME, our experiments show that CLIQUE produces local importances near zero when a variable is irrelevant and nonzero values otherwise.

2 Local Variable Importances with CLIQUE

Consider a dataset $(\mathbf{x}_1, y_1), \dots, (\mathbf{x}_n, y_n) = (X, Y)$, where $X \in \mathbb{R}^{n \times p}$ is the data matrix and $Y \in \mathbb{R}^n$ contains the labels. CLIQUE is model-agnostic and uses cross-validation (CV) predictions to compute local importances. The goal of CLIQUE is to obtain a measure of importance for the j th variable at the i th data point. Intuitively, the importance of variable j for a given data point \mathbf{x}_i in a prediction model can be measured by assessing how much the model error changes when the variable values change.

CLIQUE aims to achieve several desirable properties when assessing local importance:

- P1** If altering a variable value does not affect the model output for an observation, that variable should have an importance near 0 for that observation.
- P2** An immediate application to multi-class problems, where if altering a variable yields new predicted classes or probabilities, that variable is important regardless of the class label it has.

P3 Importance directly depends on model errors rather than predictions.

To achieve a method that offers these properties, we first build a full model using CV for hyperparameter tuning. Although training errors can be used to assess importance, test errors provide a better estimate of model performance on unseen data [19]. To capitalize on these benefits, CLIQUE computes local importance using CV errors by training multiple CV models with the same hyperparameters as the final model. Each variable is systematically modified for every data point and predictions are generated from a CV model that excluded that point from training. Comparing the CV error rate of the modified data to the original CV error rate yields a local importance measure.

Some importance measures can use only a single altered value of a variable [8]. While this approach is generally sufficient for global importance measures that average across data points, it can lead to high variance in local importance measures. To address this, local methods use multiple alterations to reduce variance [17]. Molnar suggests that the most accurate results are achieved by replacing a specific value with all other possible variable values, although this is computationally expensive [19]. We efficiently approximate this by using a quantile grid of values for each variable, spanning the variable range.

Mathematically, consider the data point \mathbf{x}_i with its corresponding CV model. We aim to compute the local importance for variable j , which we denote as V_{ij} . Let $\hat{f}(\mathbf{x}_i)$ represent the original prediction of y_i given \mathbf{x}_i as input using the CV model where \mathbf{x}_i is excluded from training. Let $\tilde{\mathbf{x}}_i(j, m)$ be the altered version of \mathbf{x}_i in which the j th variable is replaced with the m th altered value from the quantile grid. The CLIQUE value is

$$(1) \quad V_{ij} = \frac{1}{M} \sum_{m=1}^M \mathcal{L}(\hat{f}(\tilde{\mathbf{x}}_i(j, m)), y_i) - \mathcal{L}(\hat{f}(\mathbf{x}_i), y_i),$$

where M is the number of altered values in the quantile grid and \mathcal{L} is the loss function of interest (e.g. squared error in regression). A complete workflow for CLIQUE is shown in Algorithm 1. Note that $V_{:j}$ refers to the j th column in V .

We note that CLIQUE captures conditional information from the perspective that a conditional effect is present if it depends or changes upon another effect. Thus, we are not referring to conditional information in a formal probabilistic sense. We also note that for our work, “local” suggests at least some location-dependence on the importance of a variable. If there is

Algorithm 1 CLIQUE

```

1: Input: data  $X$ , labels  $Y$ , model, quantiles  $M$ 
    $n \times p$   $n \times 1$ 
2:  $mod \leftarrow \text{model}(X, Y)$ 
3:  $cvmod \leftarrow$  individual CV models
4:  $Err \leftarrow \mathcal{L}(\text{predict}(cvmod, X), Y)$ 
    $n \times 1$ 
5:  $V \leftarrow 0$ 
    $n \times p$   $n \times p$ 
6: for  $j = 1$  to  $p$  do
7:    $grid \leftarrow M$  quantile values for variable  $j$ 
    $M \times 1$ 
8:   for  $m = 1$  to  $M$  do
9:      $W \leftarrow X$ 
    $n \times p$   $n \times p$ 
10:     $W_{:j} \leftarrow m$ 
    $n \times 1$ 
11:     $\widetilde{Err}_j \leftarrow \mathcal{L}(\text{predict}(cvmod, W), Y)$ 
    $n \times 1$ 
12:     $V_{:j} \leftarrow V_{:j} + \frac{\widetilde{Err}_j - Err}{M}$ 
13:   end for
14: end for

```

no location-dependence, then local importance should be mostly redundant with global importance, which can be assessed using existing global methods.

Many global importance approaches permute variable values instead of using a grid [4, 8]. To show that using the quantile grid in CLIQUE outperforms repeated permutations, we include in our experimental results a method we refer to as Conditional Local Importance by Permutations (CLIP). CLIP and CLIQUE are nearly identical, except that CLIP performs M variable permutations to select alternative values, while CLIQUE replaces a variable with M quantile values.

3 Simulated Experiments

To demonstrate how CLIQUE outperforms the popular methods SHAP and LIME in capturing locally dependent relationships, we compare the methods on simulated data with known structures. For all analyses, we use $M = 25$ in both CLIP and CLIQUE. $M = 25$ was initially chosen based on desired qualities of the Central Limit Theorem for stabilizing estimates and reducing variance. Further exploratory analysis of the impact of M on CLIQUE values and their variance is available in Appendix A.3. For each of the following three data simulations, all features are independent and identically distributed (iid) from a uniform distribution $\mathcal{U}(-1, 1)$, and we generate 400 training observations.

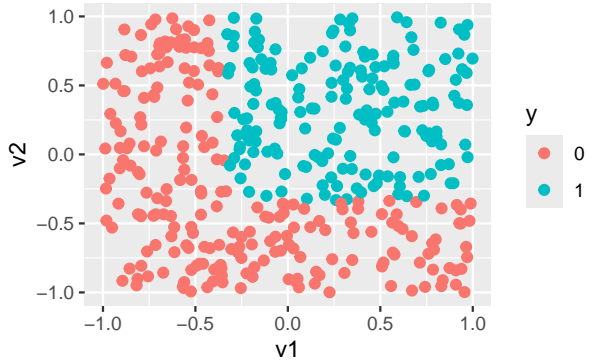


Figure 1: Scatterplot of the AND gate data colored by the label y as computed in Equation 2. When $v_2 < -1/3$, the value of v_1 should have no impact on the output of the trained model and should thus have no importance.

3.1 AND Gate Data

We begin with a simple simulation based on an AND gate (Figure 1). To create this data, we generate three features and produce the response using:

$$(2) \quad y = \begin{cases} 1, & \text{if } v_1 > -\frac{1}{3} \ \& \ v_2 > -\frac{1}{3} \\ 0, & \text{otherwise.} \end{cases}$$

Note that v_3 has no influence on the output.

We build a Random Forest model using the randomForest package [16] in the R programming language [22]. From this model, we extract SHAP values using the treeshap package [14] and also LIME values [13].

Based on the geometry of the data in Figure 1, we expect several properties for the local variable importances. When $v_2 < -1/3$, the values of v_1 should have no impact on the model output. Therefore, the v_1 importance should be close to zero when $v_2 < -1/3$. However, the values of v_1 should have large positive importance measures when $v_2 > -1/3$ due to their significant impact on the model output.

From Figure 2, we see this in the CLIQUE values. When $v_2 < -1/3$, the importance of v_1 is practically zero, while for $v_2 > -1/3$, v_1 has a positive importance. CLIP shows a similar trend, though with higher variance in the nonzero importances, highlighting the advantage of using the quantile grid in CLIQUE instead of permutations. In contrast, LIME shows no discernible difference in the importance of v_1 relative to v_2 , indicating that it fails to capture the conditional information in the data. SHAP falls between LIME and CLIQUE. It displays two distinct trends for v_1 , but still assigns nonzero importance when $v_2 < -1/3$. In other words, CLIQUE satisfies property **P1** while LIME and SHAP do not.

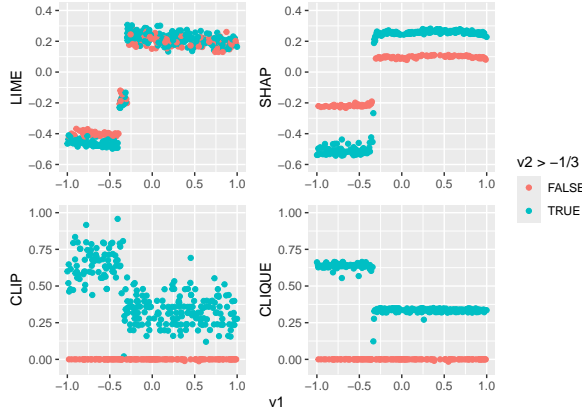


Figure 2: Scatterplots of local variable importances vs. v_1 values from the AND gate data experiment. Each plot is colored by whether $v_2 > -1/3$. CLIQUE and CLIP values output an importance of zero when $v_2 < -1/3$ and a nonzero importance otherwise. LIME values fail to distinguish between these two regions and SHAP values are nonzero when $v_2 < -1/3$.

3.2 Corners Data

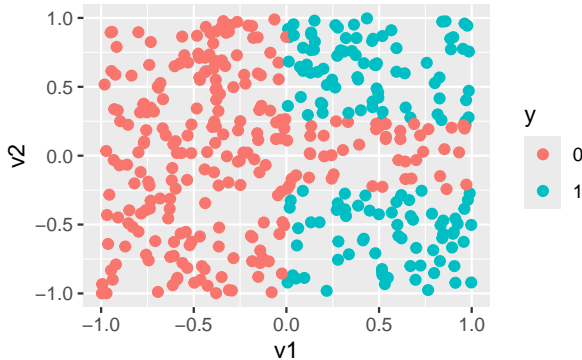


Figure 3: Scatterplot of the Corners data colored by the label y (see Equation 3). v_2 is not important when $v_1 < 0$. v_1 is not important when $|v_2| < 1/4$.

The AND Gate is a symmetric problem, where the results for v_1 mirror the results for v_2 . We now simulate values for a non-symmetric dataset that we call the Corners data (Figure 3). We generate three features with response:

$$(3) \quad y = \begin{cases} 1, & \text{if } v_1 > 0 \text{ \& } |v_2| > \frac{1}{4} \\ 0, & \text{otherwise.} \end{cases}$$

In this data, we expect that v_2 is not important when $v_1 < 0$ and v_1 is not important when $|v_2| < 1/4$. To illustrate the model-agnostic capability of CLIQUE,

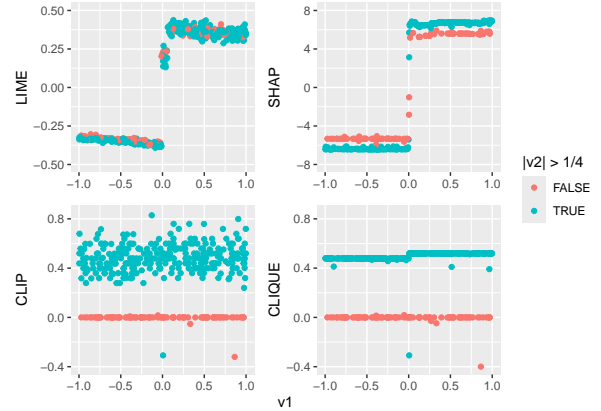


Figure 4: Scatterplots of local variable importances vs. v_1 values from the Corners data experiment. Each plot is colored by whether $|v_2| > 1/4$. As in Figure 2, the CLIQUE and CLIP values capture the known conditional relationships between v_1 and v_2 , while SHAP and LIME largely fail.

we use Generalized Boosted Modeling (GBM) on the Corners data and extract LIME, SHAP, CLIP, and CLIQUE values, which are shown in Figures 4 and 5. Again, the CLIQUE and CLIP values reflect the expected behavior, with CLIQUE showing a smaller variance than CLIP. In contrast, the LIME values again show only marginal information. SHAP values primarily highlight the marginal effects with only a small amount of conditional information. That is, CLIQUE satisfies property **P1** while LIME and SHAP do not.

3.3 Regression Interaction Data

We now turn to a location-dependent regression simulation (Figure 6) with four features that produce the response:

$$(4) \quad y = \begin{cases} v_1, & \text{if } v_3 > 0 \\ v_2, & \text{if } v_3 < 0. \end{cases}$$

In this data, v_1 should not be important when $v_3 < 0$ and v_2 should not be important when $v_3 > 0$. We build a Random Forest model and again extract LIME, SHAP, CLIP and CLIQUE values, with the results shown in Figure 7. The trends are similar to previous findings: CLIQUE satisfies **P1** while LIME and SHAP fail to do so. As in Section 3.1, SHAP values show differences between the two regions, but most values remain nonzero for the region where no v_1 importance is expected. A unique observation for this regression problem is that CLIP and CLIQUE

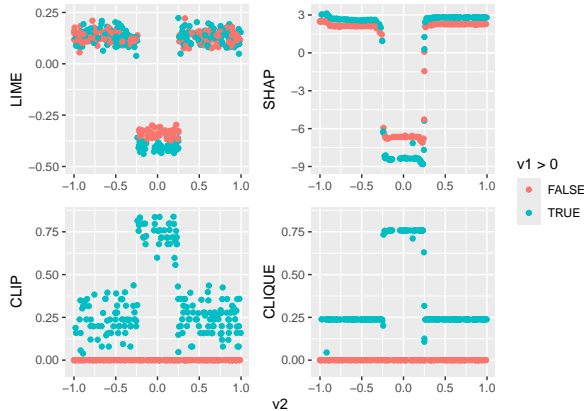


Figure 5: Scatterplots of local variable importances vs. v_2 values from the Corners data experiment. Each plot is colored by whether $v_1 > 0$. As in Figure 4, the CLIQUE and CLIP values capture the known conditional relationships between v_1 and v_2 , while SHAP and LIME largely fail.

show a quadratic relationship with data values when they are locally important.

4 Real Data Experiments

Here we apply CLIQUE to real data, including the lichen dataset [6], the MNIST dataset [1], and the concrete regression dataset [28] (see Appendix A.1).

4.1 Lichen Classification

In the lichen data, each observation is a different location in a survey region of the Pacific Northwest. This dataset consists of many climate, vegetation, and topographic features for assessing a binary response of the presence or absence of a species of lichen (*Lobaria oregana*). We build a Random Forest model using all available features, and extract LIME, SHAP, CLIP, and CLIQUE values. Results for permutation-based global variable importances [4] are shown in Figure 8. MinTempAve (minimum temperature) and ACONIF (age of conifers) are two of the most important variables for classifying the presence of Lichen. Descriptive analyses show that MinTempAve is highly collinear with AmbVapPressAve ($\rho = 0.997$) and Elevation ($\rho = -0.978$), while being mostly orthogonal to ACONIF ($\rho = -0.116$). We focus on MinTempAve, recognizing that very similar patterns will exist for AmbVapPressAve and Elevation. The ACONIF PDP shows a steady upward trend, whereas MinTempAve exhibits a plateau, followed by a steep increase, and

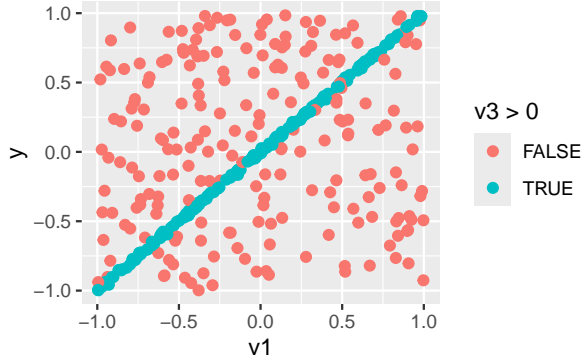


Figure 6: Scatterplot of the Regression Interaction data colored by whether $v_3 > 0$ (see Equation 4). v_1 is not important when $v_3 < 0$. v_2 is not important when $v_3 > 0$.

another plateau. We aim to determine whether the importance of ACONIF changes for different minimum temperatures.

To do this, we split our data based on if MinTempAve was below 65. The resulting boxplots in Figure 9 show that the value of the ACONIF variable has a much greater CLIQUE importance when minimum temperatures are higher. This makes sense, as lichen struggle to survive in areas with low or freezing temperatures, making ACONIF less important in those regions. If it is sufficiently warm for lichen to survive, then ACONIF influences their success greatly. The SHAP value distributions in Figure 9 show apparent differences in spread when MinTempAve is above or below 65, but the effect is more evident in the CLIQUE comparisons. Aggregate absolute SHAP values yield an impressive ratio of 3.52, while CLIQUE values yield a more outstanding aggregate absolute value ratio of 11.25.

We now demonstrate the use of CLIQUE on individual data points, with a focus on the first two observations. From Figure 10, we see that the CLIQUE value of PctVegCov is the most important for observation 1, while MinTempAve and ACONIF do not appear among the top variables. Observation 2 aligns more with the global story, having MinTempAve as the top variable and ACONIF on the list. LIME heavily emphasizes global variables here. SHAP values appear to blend the CLIQUE values of Figure 10 and the global importances from Figure 8.

4.2 MNIST Digit Classification

As another illustrative example, we analyze a downsampled version of the MNIST Digit test dataset [1] available from scikit-learn [21]. This dataset con-

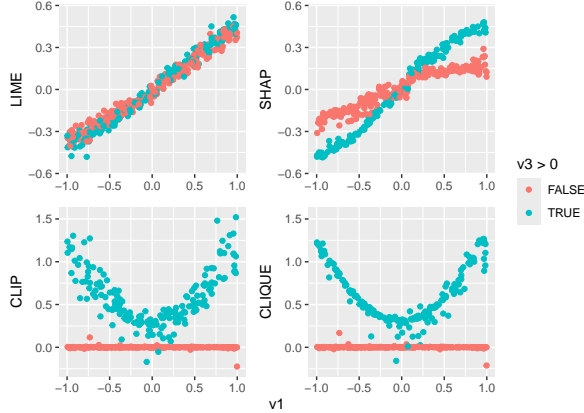


Figure 7: Scatterplots of local variable importances vs. v_1 values from the Regression Interaction data experiment. Each plot is colored by whether $v_3 > 0$. CLIQUE and CLIP capture the expected conditional relationships between variables, while LIME and SHAP largely fail.

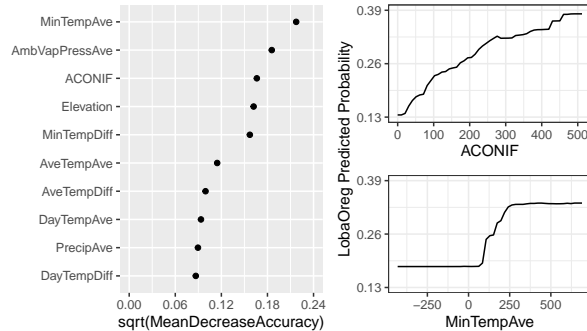


Figure 8: Global importances (left) and PDPs (right) for top features in the Lichen data.

sists of 64 features, each a pixel value, with x and y -coordinates ranging from 1 to 8. These pixel values help determine which hand-drawn digit each observation corresponds to. Since this is a multi-class problem, SHAP and LIME are not natively adapted to provide local importances. An example plot of digits is shown in Figure 11. We train a Random Forest model on this data to obtain CLIQUE values. Results for the top permutation-based global importance variables and PDPs are shown in Figure 12.

Figure 12 shows that x_{4y6} and x_{3y6} are two of the most important variables for classifying digits and they neighbor each other. The x_{4y6} PDP in Figure 12 shows a distinct region of changing probabilities for low values followed by a plateau effect after about 4.5. The x_{3y6} PDP shows a clear crossing pattern at a value of about 7.5. These results suggest the

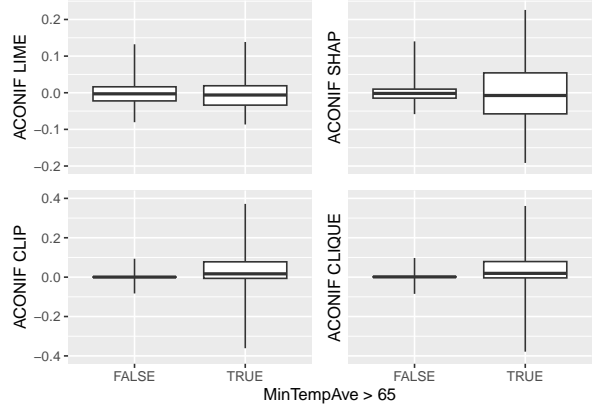


Figure 9: Distributions of ACONIF importances for different MinTempAve thresholds. Classically defined outliers are included in whiskers. The CLIQUE values show a greater contrast between the two regions compared to the other methods.

possibility that x_{4y6} may be more or less important for low or high values of x_{3y6} . They especially imply that x_{3y6} may be more or less important for low or high values of x_{4y6} .

The boxplots in Figure 13 show that x_{4y6} has a greater importance when x_{3y6} is less than 7.5, while x_{3y6} has a greater importance when x_{4y6} is less than 4.5. These results imply an interaction between these pixels, where each pixel value is more important when the other has a lower value. This behavior is similar to results seen in the AND Gate data of Section 3.1.

In addition to comparing pixel importances against pixel values, we also compare them across digit labels. We present this from two different perspectives. The first is found in Figure 14 which shows CLIQUE boxplots grouped by labels, effectively illustrating that CLIQUE satisfies property **P2**. Pixel x_{4y6} has noticeably higher CLIQUE values for the digits 3 and 9. Although initially surprising, further analysis reveals that for digits 3 and 9, x_{4y6} equals 0 more than 80% of the time, while for other digits, it equals 0 less than 60% of the time. Therefore, a value of 0 strongly indicates that a digit is likely a 3 or 9, whereas a value above 0 suggests otherwise.

Figure 14 also shows that x_{3y6} has particularly high CLIQUE values for digits of 5, 6, 8, and 9. These results align well with intuition, as common sense suggests x_{3y6} would show strong differences between digits 5 and 6. It is also expected to be a key pixel for distinguishing between digits 8 and 9.

The second perspective uses a dimensionality reduction method known as PHATE [20]. PHATE is a visualization tool that balances global and local

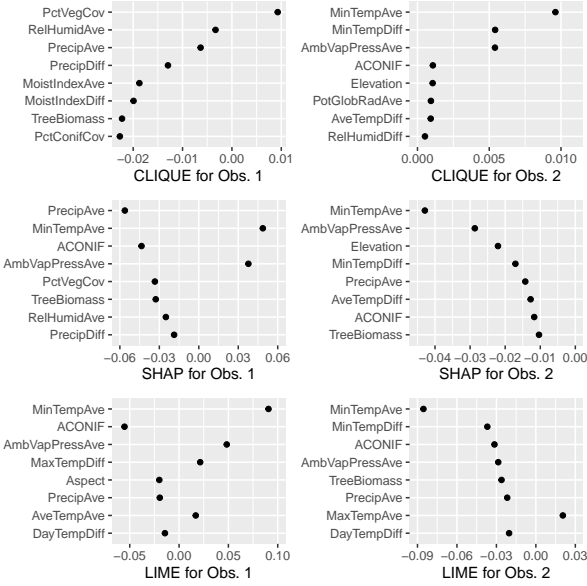


Figure 10: CLIQUE, SHAP, and LIME values of top 8 features for two instances in the Lichen data. Based on the CLIQUE values, the first observation has different important variables than the second observation, which tends to match the global trends.

structures in data. Here, we reduce the data down to two dimensions and create scatterplots of those dimensions in Figure 15. We color this plot by class labels and discretized CLIQUE categories to identify further trends and patterns in our data. From Figure 15, PHATE appears to separate the data into 12 natural clusters, which mostly align with the digit labels, with class 1 and 9 being split.

Beginning with x_4y_6 in Figure 15, we can see that low CLIQUE values tend to be in the bottom-left quadrant of the plot. High CLIQUE values tend to fit into the top-right section. Generally, digits 3 and 9 show high values, while digits 0 and 6 show low. One digit class especially catches our attention though: the number 5. Its cluster shows up as a gradient with low CLIQUE values in the top section and high CLIQUE values in the bottom. This suggests that x_4y_6 CLIQUE values may be a good metric for sorting images of the number 5.

Surprisingly, x_3y_6 highlights opposing regions in Figure 15. High CLIQUE values generally appear in the bottom right quadrant, while low values fall in the top left. We can visually see that digits 2, 4, and 7 show low values, while digits 5, 6, and 9 show high values. The digits 3 and 9 have overlapping groups, yet we can fairly distinguish them by whether their x_3y_6 CLIQUE value was high or low. As mentioned earlier,

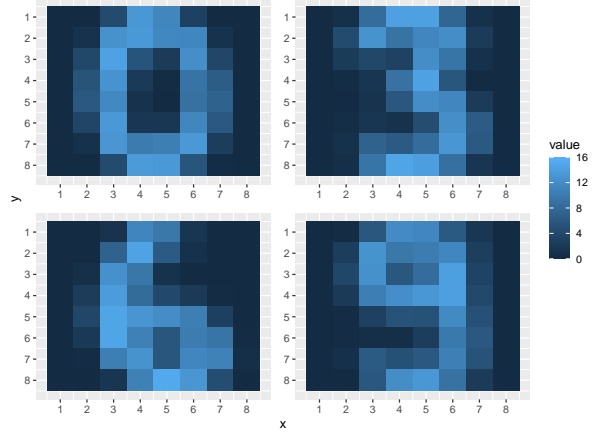


Figure 11: Aggregate tile plots for four digits from the down-sampled MNIST Digit test data. Pixel values are averaged across each observation of a particular digit class to generate these plots.

the number 1 is split into two separate groups. The CLIQUE values of x_3y_6 appear to be a good metric for comparing these groups. The top-right cluster has strictly high CLIQUE values for x_3y_6 , while the larger main group tends to have lower CLIQUE values. This shows that x_3y_6 or its CLIQUE values may be a useful metric for parsing out this subgroup structure. See the Appendix for additional results.

5 Discussion and Conclusion

CLIQUE offers a unique perspective on local importance, highlighting and emphasizing conditional or locally dependent information that SHAP and LIME do not provide with the same degree of focus.

While this paper focuses on comparing the values themselves, we acknowledge that computation speed is often a key consideration. Time-cost comparison plots and analysis can be found in Appendix A.4. From this analysis we found that SHAP and CLIQUE are noticeably faster than LIME. Additionally, CLIQUE scales linearly with more observations, which is better than the quadratic scaling found in SHAP. Conversely, SHAP scales roughly constant with respect to the number of feature, which is superior to the linear scaling of CLIQUE. The current version of CLIQUE is competitive with SHAP and LIME, with room for further improvements.

In assessing the local importances, we observe that LIME values consistently tend to capture marginal information exclusively. This is not surprising, since LIME tends to be focused on explaining individual

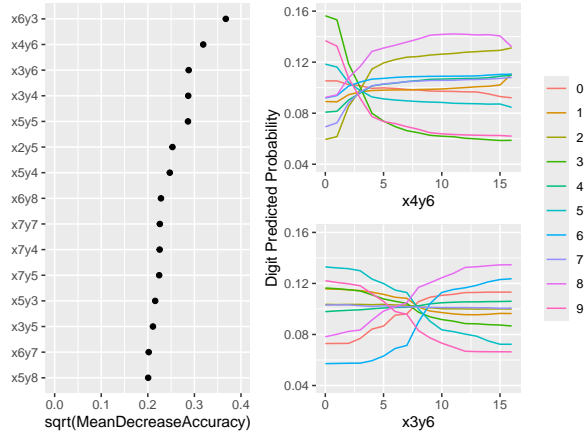


Figure 12: Global importances (left) and Partial Dependence Plots (right) for top features in the down-sampled MNIST Digits test data.

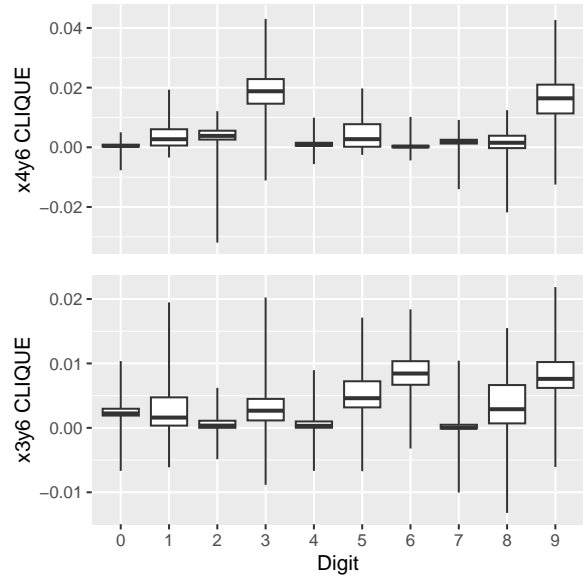


Figure 14: Distributions for $x4y6$ and $x3y6$ CLIQUE values across digit classes. Classically defined outliers are included in whiskers, rather than as distinct points.

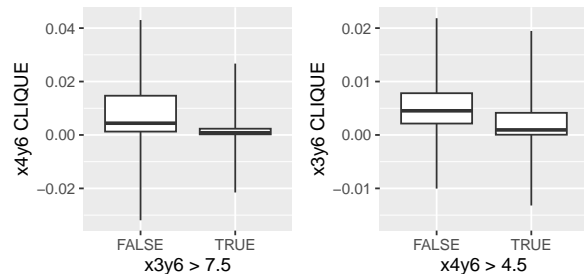


Figure 13: Distributions for $x4y6$ and $x3y6$ CLIQUE values across identified cutoffs. Classically defined outliers are included in whiskers. These results imply an interaction between these pixels, where each pixel value is more important when the other has a lower value.

predictions, and is rarely applied globally as we have done here. SHAP offers a combination of marginal and conditional information, mostly showing the marginal trend, but also sometimes splitting out conditional groups. SHAP also preserves directions and magnitudes, providing immediate insights about how a variable value contributes to a prediction. Positive values imply an increase to an average prediction, while negative values imply a decrease. Global assessments for SHAP are done on the spread of the values, not the center, because the centers are zero.

CLIQUE is highly conditional, measuring how a variable value affects prediction error rather than the prediction itself. Near-zero values indicate no effect on individual error, while positive values suggest the variable is important for reducing it. Global assessments can potentially be made from the centers and

spreads of CLIQUE values. We note that if a variable is more important in one location, the center and the spread of the CLIQUE values will be higher in that location.

These three methods appear analogous to different regression concepts. LIME is reminiscent of building a model using only one variable at a time. SHAP parallels constructing a model that includes all variables and possibly some interactions. CLIQUE resembles partial residuals or partial effects, which account for the contributions of other variables before evaluating a variable of interest.

In summary, we have provided the structure for a new and novel local importance algorithm. We have shown many applications and contributions of CLIQUE, including its powerful use in capturing conditional or locally dependent importances, improvement over permutation-based methods, and direct use in multi-class classification problems. This research offers many future opportunities for expansion into global importance methods and improving permutation-based algorithms generally.

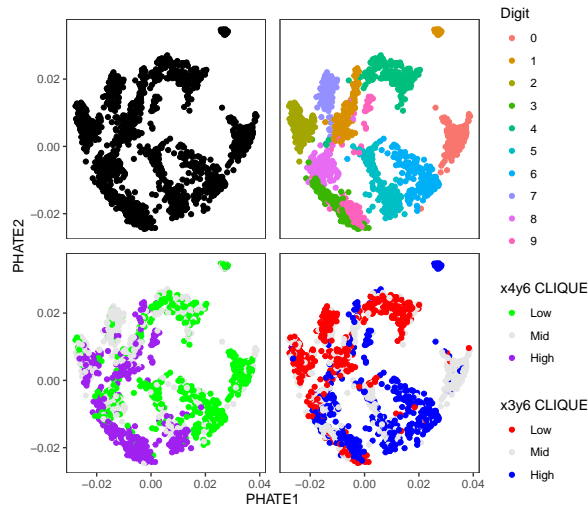


Figure 15: Scatterplots of PHATE embeddings for the MNIST Digit data. Top-Left: Default plot. Top-Right: PHATE colored by actual digit classes. Bottom-Left: PHATE colored by x4y6 importances cut into three equally sized bins. Bottom-Right: PHATE colored by x3y6 importances cut into three equally sized bins. Digits 3 and 9 have comparably higher x4y6 CLIQUE values, while digits 5, 6, and 9 have comparably higher x3y6 CLIQUE values.

References

- [1] E. Alpaydin and C. Kaynak. Optical recognition of handwritten digits. UCI Machine Learning Repository, 1998. DOI: <https://doi.org/10.24432/C50P49>.
- [2] Rina Foygel Barber and Emmanuel J Candès. Controlling the false discovery rate via knockoffs. *The Annals of statistics*, pages 2055–2085, 2015.
- [3] Kelvyn Bladen and D Richard Cutler. Assessing agreement between permutation and dropout variable importance methods for regression and random forest models. *Electronic Research Archive*, 32(7):4495–4514, 2024.
- [4] Leo Breiman. Random forests. *Machine learning*, 45(1):5–32, 2001.
- [5] Emmanuel Candès, Yingying Fan, Lucas Janson, and Jinchi Lv. Panning for gold: ‘model-x’ knockoffs for high dimensional controlled variable selection. *Journal of the Royal Statistical Society Series B: Statistical Methodology*, 80(3):551–577, 2018.
- [6] D Richard Cutler, Thomas C Edwards Jr, Karen H Beard, Adele Cutler, Kyle T Hess, Jacob Gibson, and Joshua J Lawler. Random forests for classification in ecology. *Ecology*, 88(11):2783–2792, 2007.
- [7] Susanne Dandl, Christoph Molnar, Martin Binder, and Bernd Bischl. Multi-objective counterfactual explanations. In *International conference on parallel problem solving from nature*, pages 448–469. Springer, 2020.
- [8] Aaron Fisher, Cynthia Rudin, and Francesca Dominici. All models are wrong, but many are useful: Learning a variable’s importance by studying an entire class of prediction models simultaneously. *Journal of Machine Learning Research*, 20(177):1–81, 2019.
- [9] Alex Goldstein, Adam Kapelner, Justin Bleich, and Emil Pitkin. Peeking inside the black box: Visualizing statistical learning with plots of individual conditional expectation. *journal of Computational and Graphical Statistics*, 24(1):44–65, 2015.
- [10] Brandon M. Greenwell. pdp: An R package for constructing partial dependence plots. *The R Journal*, 9(1):421–436, 2017.
- [11] Brandon M Greenwell, Bradley C Boehmke, and Andrew J McCarthy. A simple and effective model-based variable importance measure. *arXiv preprint arXiv:1805.04755*, 2018.
- [12] Giles Hooker, Lucas Mentch, and Siyu Zhou. Unrestricted permutation forces extrapolation: variable importance requires at least one more model, or there is no free variable importance. *Statistics and Computing*, 31:1–16, 2021.
- [13] Emil Hvitfeldt, Thomas Lin Pedersen, and Michaël Benesty. *lime: Local Interpretable Model-Agnostic Explanations*, 2022. R package version 0.5.3.
- [14] Konrad Komisarczyk, Pawel Kozminski, Szymon Maksymiuk, and Przemyslaw Biecek. *treeshap: Compute SHAP Values for Your Tree-Based Models Using the ‘TreeSHAP’ Algorithm*, 2024. R package version 0.3.1.
- [15] Jing Lei, Max G’Sell, Alessandro Rinaldo, Ryan J Tibshirani, and Larry Wasserman. Distribution-free predictive inference for regression. *Journal of the American Statistical Association*, 113(523):1094–1111, 2018.
- [16] Andy Liaw and Matthew Wiener. Classification and regression by randomforest. *R News*, 2(3):18–22, 2002.

- [17] Scott Lundberg. A unified approach to interpreting model predictions. *arXiv preprint arXiv:1705.07874*, 2017.
- [18] Scott M Lundberg, Gabriel G Erion, and Su-In Lee. Consistent individualized feature attribution for tree ensembles. *arXiv preprint arXiv:1802.03888*, 2018.
- [19] Christoph Molnar. *Interpretable machine learning*. Lulu.com, 2020. Chapter 8.5 and Chapter 9, accessed: 2025-01.
- [20] Kevin R Moon, David Van Dijk, Zheng Wang, Scott Gigante, Daniel B Burkhardt, William S Chen, Kristina Yim, Antonia van den Elzen, Matthew J Hirn, Ronald R Coifman, et al. Visualizing structure and transitions in high-dimensional biological data. *Nature biotechnology*, 37(12):1482–1492, 2019.
- [21] F. Pedregosa, G. Varoquaux, A. Gramfort, V. Michel, B. Thirion, O. Grisel, M. Blondel, P. Prettenhofer, R. Weiss, V. Dubourg, J. Vanderplas, A. Passos, D. Cournapeau, M. Brucher, M. Perrot, and E. Duchesnay. Scikit-learn: Machine learning in Python. *Journal of Machine Learning Research*, 12:2825–2830, 2011.
- [22] R Core Team. *R: A Language and Environment for Statistical Computing*. R Foundation for Statistical Computing, Vienna, Austria, 2022.
- [23] D Rene. Coarse-grained 6x6 pixel mnist dataset, 2025. MATLAB Central File Exchange, Retrieved: 2025-01.
- [24] Marco Tulio Ribeiro, Sameer Singh, and Carlos Guestrin. "why should i trust you?" explaining the predictions of any classifier. In *Proceedings of the 22nd ACM SIGKDD international conference on knowledge discovery and data mining*, pages 1135–1144, 2016.
- [25] Marco Tulio Ribeiro, Sameer Singh, and Carlos Guestrin. *Anchors: High-precision model-agnostic explanations*, 2018.
- [26] Lloyd S Shapley et al. *A value for n-person games*, 1953.
- [27] Sandra Wachter, Brent Mittelstadt, and Chris Russell. Counterfactual explanations without opening the black box: Automated decisions and the gdpr. *Harv. JL & Tech.*, 31:841, 2017.
- [28] I-Cheng Yeh. Concrete Compressive Strength. UCI Machine Learning Repository, 1998. DOI: <https://doi.org/10.24432/C5PK67>.

A Additional Experiments

Here we include additional results from a regression dataset for predicting Concrete Strength [28]. We also show extended results from the MNIST digit classification dataset, analyze the effect of M , and compare the computational cost of CLIQUE with SHAP and LIME.

A.1 Concrete Regression

To illustrate an application for our method in regression, we use the Concrete Compressive Strength data [28]. This dataset is available on the UCI data repository and consists of 1030 observations. There are eight quantitative ingredients or features and a response listed with their respective units as: Cement (kg/m^3), Blast Furnace Slag (kg/m^3), Fly Ash (kg/m^3), Water (kg/m^3), Superplasticizer (kg/m^3), Coarse Aggregate (kg/m^3), Fine Aggregate (kg/m^3), Age (days), and Concrete Compression Strength (MPa).

With this data, we build a Random Forest model and extract LIME, SHAP, CLIP and CLIQUE values from it. Results for permutation-based global variable importances and PDPs are shown in Figure 16.

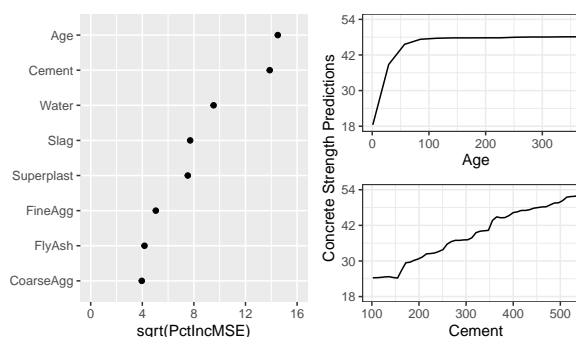


Figure 16: Left: Global importances for all features in the Concrete data. Right: PDPs for Age and Cement, the top two features.

Figure 16 shows that Age and Cement appear to be the most important ingredients for determining Concrete Strength. We especially notice that the Cement PDP shows a fairly consistent trend upward. Conversely, the Age PDP shows Strength predictions initially rising rapidly, but then stabilizing at an Age between 50 and 100 days. These results raise the question: Does Cement importance change for different Ages?

To answer this question, we manually cut our local importances into two groups based on whether the Age exceeded 75 days or not. The CLIP and CLIQUE boxplots in Figure 17 show that Cement has

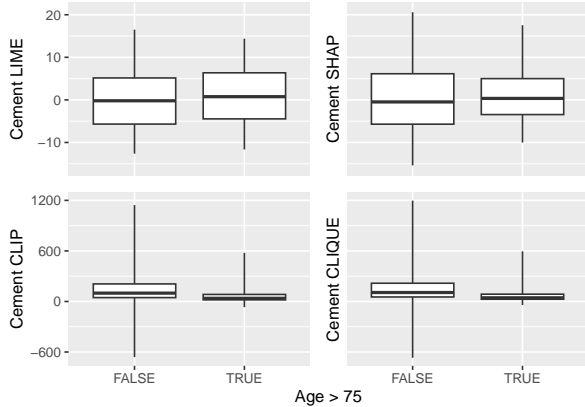


Figure 17: Distributions for Cement importances for different Age thresholds. Classically defined outliers are included in whiskers. The CLIQUE values show a greater contrast between the two regions compared to LIME and SHAP.

a greater importance when Ages are lower. In other words, concrete strength accuracy is more influenced by cement amount if the age is lower. Little difference is observed in the LIME values, while the SHAP values in Figure 17 do show a slightly larger spread when Age is less than 75. This effect is diminished greatly compared to the difference seen in the CLIP and CLIQUE distributions. Aggregate SHAP values, calculated by averaging the SHAP magnitudes, yield a ratio of 1.36, whereas the mean of the CLIQUE values produces a ratio of 2.15 times higher for lower ages compared to higher ages.

This dataset again poses an excellent opportunity to extract individual importance metrics. In Figure 18, we show CLIQUE, SHAP, and LIME values for two observations, the first and the third instances of the concrete dataset.

From Figure 18, we see that the value of Cement has the strongest implications for observation 1. In fact, when looking at Figure 17, we see that the cement importance for observation 1 is the highest local importance achieved. The LIME and SHAP values for cement are high, which, when coupled with the cement PDP from Figure 16, implies that the Cement value is high.

In contrast, observation 3 does not have Cement as a top contributing variable. It shows that Water, Superplasticizer, and Age are most important for determining Strength correctly. The SHAP and LIME values generally agree with this, although they give higher priority to Age due to its stronger global influence. We especially note that the scales for the plots do not match, except perhaps for LIME. Water

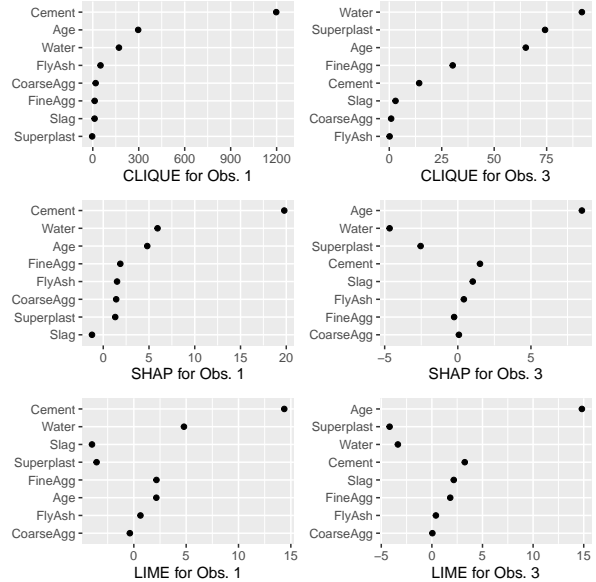


Figure 18: CLIQUE, SHAP, and LIME values of all predictor variables for two instances in the Concrete data. Based on the CLIQUE values, the first observation has very different important variables than the third observation, which deviates substantially from the global trends.

has a CLIQUE value of nearly 200 for observation 1, while only having a value of 90 for observation 3. This makes sense when considering the context that observation 3 is the 63.8 percentile of the response while observation 1 is the 99.6 percentile.

A.2 Additional MNIST Results

In the MNIST example from Section 4.2, we explore CLIQUE importances for pixels. We now take a different approach of assessing top pixels across each digit class. This is done by calculating the mean CLIQUE value for each pixel across each class. We collect the top five pixels for each class and show them in Figure 19.

From Figure 19, we see that no pixels containing x1 or x8 ever show up. This matches trends in Figure 11, where we see those two columns of pixels are always zero for each of the example digits.

We also observe that digits 3 and 9 share x4y6 as their top pixel. In Section 4.2, we observed that the distribution of x4y6 CLIQUE values stood out drastically for these two digits.

Meanwhile, digits 5 and 6 both share x6y3 as their most important pixel. This was followed by x3y6, which we discuss in Section 4.2 as a strong discriminator for these digits. x6y3 does not seem like a

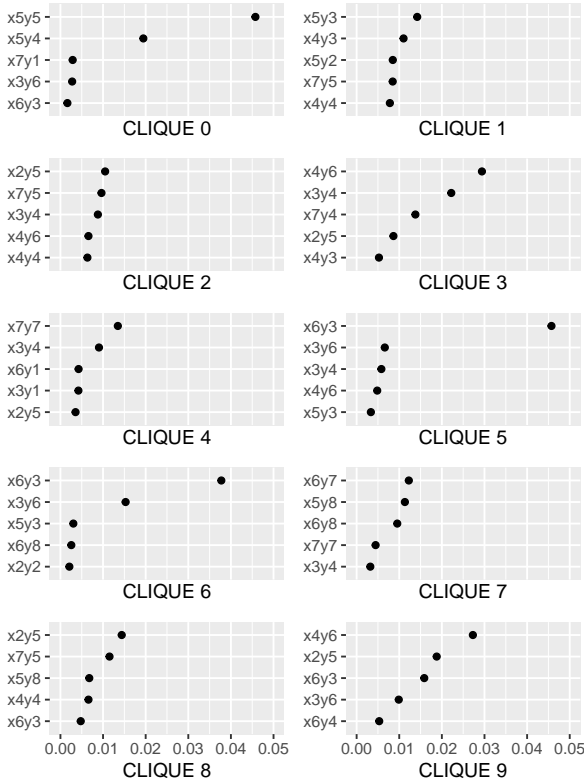


Figure 19: Plot showing top 5 predictor variables based on mean CLIQUE values for each digit class. Using the CLIQUE values, digits can be identified that benefit from globally important pixels of $x4y6$ and $x6y3$.

powerful pixel for splitting 5s and 6s, since both digits tend to have low values for this pixel. However, it is very effective for splitting 5s and 6s into their own cluster, away from the remaining digits, which generally have high values for $x6y3$. A noteworthy takeaway is that CLIQUE importance is focused on how a value compares to the whole distribution of that variable. If eight classes have a high pixel value, while two have a low value, that pixel will be very important for the two different classes, but not as important for the other eight.

We can see this in digit 0, which has a very high CLIQUE value for $x5y5$ and $x5y4$. Despite this, both pixels never show up in the top five pixels for any other digit. A likely reason is that these pixel values are low for 0, but higher for all other digits on average. Thus, 0 is an anomalous digit for these pixels, which makes them excellent at splitting 0s from the rest of the digits.

In addition to considering top pixels across digit classes, we also further explore the two PHATE

clusters for digit 1. We select central points from these clusters, visualize them, and compare their top CLIQUE pixels in Figure 20.

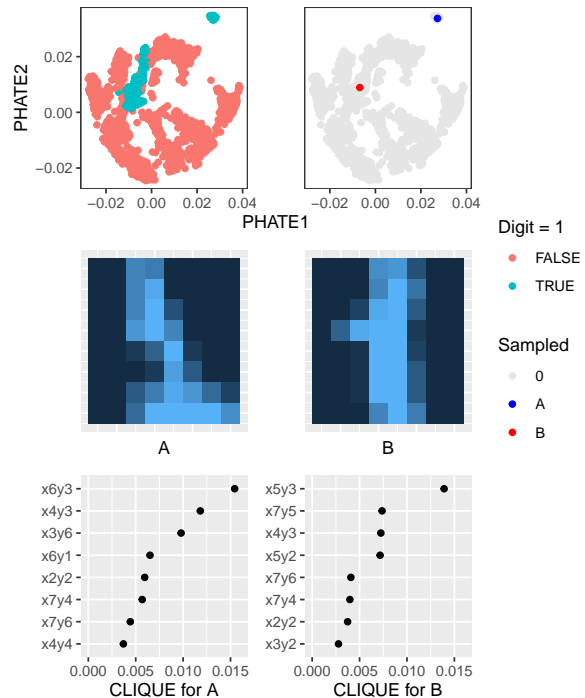


Figure 20: Plot showing samples from both digit 1 PHATE clusters. Top-Left: PHATE colored by digit 1 class. Top-Right: PHATE colored by samples A and B. Middle: Tile plot of A and B. Bottom: Top 8 pixels from CLIQUE values for A and B.

From Figure 20, we find that the points labeled A and B share many of the same top pixels identified by CLIQUE. Both samples show that $x4y3$, $x7y4$, $x2y2$, and $x7y6$ are quite important. Even though the sample images look very different, (A has an underline while B does not), these identified pixels show similar trends. The value of $x4y3$ is high in both images, while $x7y4$, $x2y2$, and $x7y6$ have low values in both images.

CLIQUE is useful for identifying pixels that help distinguish these digit 1 samples from other digits. While samples A and B share a value of 0 for $x1y1$, it is not important because most digits also have a value of 0. In contrast, $x4y3$ has a much higher value for digit 1 compared to most other digits. Both samples A and B have high values for $x4y3$, making it locally important. The digit 1 also shows much higher values for $x5y3$ compared to other digits. For sample B, this digit is very important due to its high value. However, sample A has a much lower value for $x5y3$, making $x5y3$ much less important for assisting in its

classification.

A.3 Analyzing the effect of M

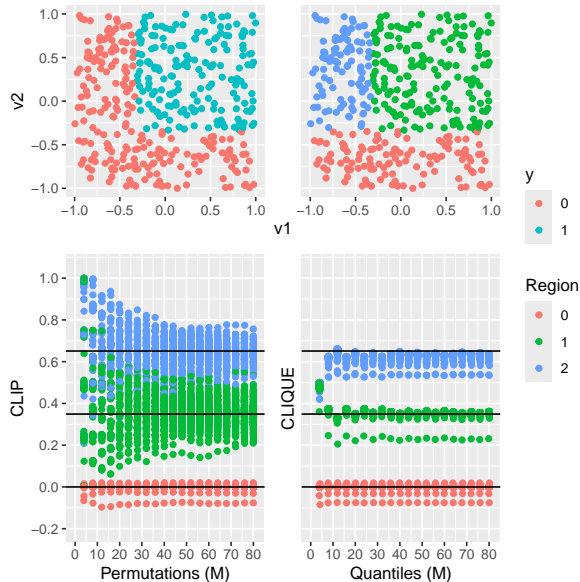


Figure 21: Plot showing panels of data scatterplots and the relationship between importance value distributions and the hyper-parameter M . Top-Left: Scatter-plot showing $V1$ and $V2$, colored by the response (y). Top-Right: Scatter-plot showing $V1$ and $V2$, colored by regions of interest with respect to $V1$. Bottom-Left: Plot showing the distribution of CLIP values across the hyper-parameter M , colored by regions. Bottom-Right: Plot showing the distribution of CLIQUE values across the hyper-parameter M , colored by regions. The CLIQUE values have a smaller spread for each value of M .

We used the data structure from Section 3.1 to examine the effect of M on CLIQUE values. Recall that M represents the number of altered values in the quantile grid. To demonstrate some of the advantages that CLIQUE has over permutation-based methods to assessing local importance, we also run the same experiments using CLIP, where M represents the number of permuted values used to assess the importance.

The results are shown in Figure 21. Consistent with our previous experiments, these results show that the CLIP values have a much larger spread than the CLIQUE values in each region of interest.

The results in Figure 21 also provide guidance on selecting an appropriate M . As noted in Section 3, we chose $M = 25$ to stabilize estimates and reduce variance. Figure 21 reveals that CLIQUE value variances

remain remarkably consistent across all M , while the value centers show some initial volatility before stabilizing around $M = 15$. Beyond this point, higher M values provide diminishing returns at an increased computational cost.

Considering these findings alongside the stability observed in Section 3, we suggest that M values between 20 and 50 are generally conservative enough to yield stable estimates. However, larger M values may be warranted for datasets with highly complex interactions or decision boundaries.

A.4 Time Cost Comparison

Here we performed a computational time comparison between CLIQUE, SHAP, and LIME. We used the MNIST dataset with images aggregated to a 6x6 pixel resolution [23] to test the effects of increasing both the number of observations and the number of features on computational time. To ensure compatibility with both SHAP and LIME (which are adapted natively only to binary classification), we limited the dataset to just two digit classes: 3 and 8. These comparisons were all conducted on a Windows computer with an AMD Ryzen 7 4700U 2.00 GHz processor, featuring 8 cores and 16 GB of RAM.

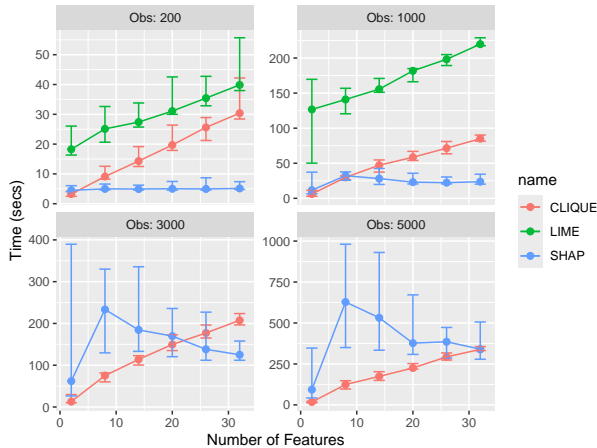


Figure 22: Plot showing computation time results as features increase, faceted by observations. The points and error bars represent the minimum, median, and maximum times from 12 Monte Carlo simulations.

Figure 22 shows the computational time in seconds for all three methods as a function of the number of features and for different sample sizes. From these results, we observe that both SHAP and CLIQUE are significantly faster than LIME. Additionally, the figure reveals that the SHAP runtime is approximately independent of the number of features, although the

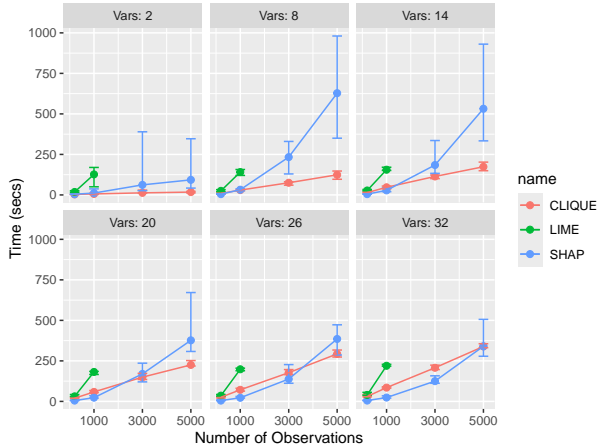


Figure 23: Plot showing computation time results as the number of observations increase, faceted by variables. The points and error bars represent the minimum, median, and maximum times from 12 Monte Carlo simulations.

variance can be high. In contrast, the CLIQUE runtime increases linearly with the number of features and is more stable.

Figure 23 shows the same results with the computational time as a function of sample size across different numbers of features. From these results, we observe that the SHAP runtime generally increases quadratically with the number of observations, while the CLIQUE runtime remains linear.

These results suggest that CLIQUE scales better with increasing observations, while SHAP scales better with more features. This aligns with the expectations set by the authors of TreeSHAP [18], who describe a fast SHAP implementation with time complexity $O(TLD^2)$, where T is a model hyperparameter, L is the maximum number of tree nodes (which is largely dependent on the number of observations n), and $D = \log(L)$. Notably, the SHAP time complexity does not depend on the number of features p , implying that computational cost remains roughly constant across different values of p . While p does influence L , this relationship is not monotonic and is significantly weaker than the effect of n .